



## Wettability designing by ZnO periodical surface textures

Yinmin Zhang<sup>a</sup>, Ding Lan<sup>a</sup>, Yuren Wang<sup>a,\*</sup>, He Cao<sup>a</sup>, Yapu Zhao<sup>b</sup>

<sup>a</sup> Key Laboratory of Microgravity, Institute of Mechanics, Chinese Academy of Sciences, Beijing 100190, China

<sup>b</sup> State Key Laboratory of Nonlinear Mechanics, Institute of Mechanics, Chinese Academy of Sciences, Beijing 100190, China

### ARTICLE INFO

#### Article history:

Received 12 May 2010

Accepted 20 July 2010

Available online 25 July 2010

#### Keywords:

ZnO microbowl

Contact angle

Polystyrene sphere

Monolayer colloidal crystal

### ABSTRACT

A facile and effective aqueous chemical synthesis approach towards well control of periodical ZnO textures in large-scale areas is reported, by which considerable adjusting of surface wettability can be realized. With the assistance of polystyrene spheres monolayer template and morphology control agent, we succeeded in preparing a series of ordered ZnO microbowls with different sag height. It was found that the contact angle could be well adjusted by changing geometry of microbowl. Such novel, ordered arrays are expected to exploit the great potentiality in waterproof or self-cleaning micro/nanodevices, and even microfluidic devices.

© 2010 Elsevier Inc. All rights reserved.

### 1. Introduction

Wettability is an important surface property of material and wettability improvement has significant value both in fundamental research and in industrial application [1–3]. In the past several decades, the research was focused particularly on superhydrophobicity [4–9]. In another aspect, well-controlled wetting surface, characterized by specific contact angle (CA) or variable CA, is a prerequisite for many applications such as liquid transportation, waterproof, microfluidic devices [10–13]. However, the research in this direction is rare against large amount of publications on superhydrophobicity.

The wettability of a solid surface is mainly determined by the solid surface free energy and the surface micromorphology. The surface free energy is strongly related to the chemical composition and arrangement of outermost atom or atomic group of the surface [14]. Chemical surface modification can change the surface free energy, and then effectively govern the surface wettability. But it is hard to get a stable hydrophobic surface through chemical surface modification when a fresh surface was exposed in air for some time. Against of surface free energy, the surface morphology can be artificially modified that was demonstrated to be an effective way to influence the wettability [15,16]. Nowadays, the surface-structure modification has become a crucial means to obtain hydrophobic surface. Chen et al. [17] reported nanostructured TiO<sub>2</sub> surfaces with wetting properties being capable of varying from hydrophilicity to superhydrophobicity. Han's group [18] fab-

ricated several ZnO superhydrophobic surfaces utilizing oxidation reaction between zinc powder and hydrogen dioxide to produce multi-scale structures from microstructure to micronanobinary structure. Jiang's group [19–21] had done excellent research on bioinspired design of superhydrophobic interface. However, it still leaves a big challenge to design and produce a surface with a definite CA, especially through a low-cost and high-efficiency technology. Although lithography technology can be used to process the solid surface in ultraprecision, the high cost and low efficiency impeded its application in industry. Therefore, a simple, low-cost and environmentally benign method is necessary to be developed.

In the viewpoint of micro-scale structure, a droplet cannot contact completely with a solid surface due to the influence of surface roughness and surface tension. According to Cassie and Baxter [16], the contact area between a liquid droplet and a solid surface can be divided into two parts, namely, a solid wetting part and the rest airy non-wetting part. The solid wetting part is the region where the liquid can well engulf the asperities. The fractional area of the solid part is denoted as  $f_1$ . The airy non-wetting part refers to the region where the trapped air separates the liquid droplet from the protruded solid surface. The fractional area of this airy part is expressed as  $f_2$ . From Cassie equation (Eq. (1)) [22], the CA ( $\theta_r$ ) increases with decrease of solid fraction ( $f_1$ ). Here,  $\theta_r$  and  $\theta_o$  represent the CA on a rough surface and the ideal CA without considering the surface roughness. Eq. (1) can also be expressed by Eq. (2) because  $f_1 + f_2 = 1$ . It is obviously indicated that  $f_1$  plays an important role in determining CA. A solid surface with definite CA can be obtained if  $f_1$  can be adjusted in a relatively precise way.

$$\cos \theta_r = f_1 \cos \theta_o - f_2 \quad (1)$$

$$\cos \theta_r = f_1 (\cos \theta_o + 1) - 1 \quad (2)$$

\* Corresponding author. Fax: +86 010 82544096.

E-mail address: wangyr@imech.ac.cn (Y. Wang).

However, it is not easy to control the value of  $f_1$  accurately. Lithography technology can satisfy the demand for accurate manufacture, yet the high cost and low efficiency are its vital drawback in practice. In this paper, ZnO film with highly-ordered bowl-like surface pattern was successfully fabricated via an aqueous chemical synthesis method. It is convenient to regulate the parameter  $f_1$  by simply adjusting the sag height of the concave spherical crown. It should be noticed that the value of  $f_1$  is sensitive to the sag height. Therefore, a small change of sag height can induce a relatively large deviation of CA. As an important functional material [23–31], ZnO has abundant crystal morphologies and the growth of ZnO is able to be well controlled, which are favorable for realizing our strategies.

## 2. Material and methods

All chemicals (Sinopharm Chemical Reagent Beijing Co., Ltd.) were of analytical reagent grade. All the aqueous solutions were prepared using deionized water. Glass slides were used as substrates and cleaned by standard procedures prior to use. The water for contact angle test was ultra pure water (Milli-Q 18.2 M $\Omega$  cm, Millipore system). Polystyrene sphere (PS) suspensions were bought from Thermo Fisher Scientific Inc. The average diameter of PS is 1000 nm and the solids mass fraction in the suspensions is 10% by weight.

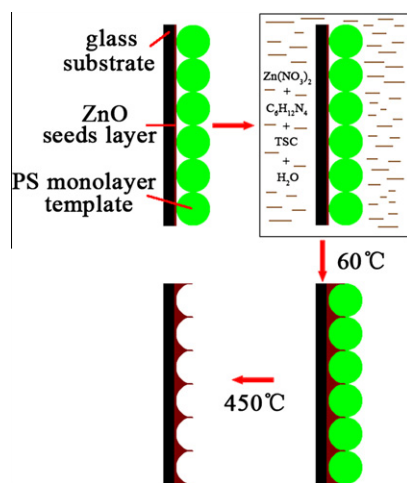


Fig. 1. Schematic illustration of the synthesis process of ZnO periodical structures.

The ZnO nanocrystals were prepared according to Meulenkamp's method [32], while the ZnO seeds layer was prepared on the glass substrate by dip coating method. The substrate was annealed at 450 °C to burn out the residual organic materials and obtain well-crystallized ZnO film.

Large-scale PS monolayer colloidal crystals (>1.5 cm<sup>2</sup> in area) were prepared by an air–liquid–solid interface self-assembly method [33]. The PS monolayer was deposited on the substrate coated with ZnO seeds layer. More details are as follows: PS suspensions were diluted with equal volume of ethanol, and then the mixed suspensions were slowly syringed on the surface of deionized water. Colloidal spheres monolayer was formed on the surface of water due to the surface tension of water. The monolayer was transferred onto the substrate when it was drawn out slowly from the suspensions by a computer-controlled linear actuator. Typically, the lift-up rate was 20  $\mu\text{m s}^{-1}$ . As the evaporation of water at the meniscus which is the interface between the substrate and the PS-monolayer-floating suspension, an attractive capillary force was formed between the neighboring spheres and played a positive role to assemble the colloidal spheres into ordered structure. Therefore, steady water evaporation rate and lift-up rate are crucial to the formation of homogenous ordered structure. Finally, the PS monolayer templates were treated at 90 °C for 15 min in order to enhance the adhesion between PS particles and ZnO seeds layer.

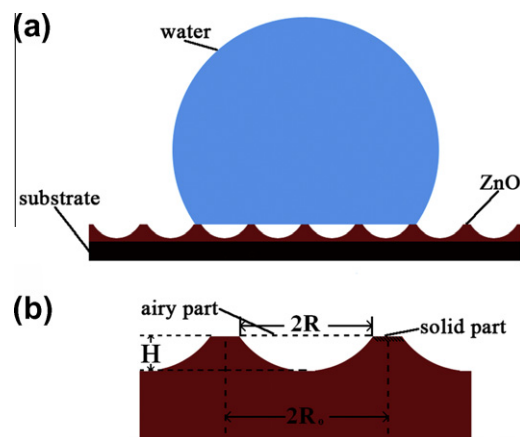


Fig. 3. Schematic illustrations of the ZnO surface wettability. (a) The shape of water on ZnO surface patterned with periodical microbowl structures and (b) the structure of a single bowl. Let  $R_0$  be the radius of one PS, and let  $R$  denote the radius of the top edge of the concave spherical crown.

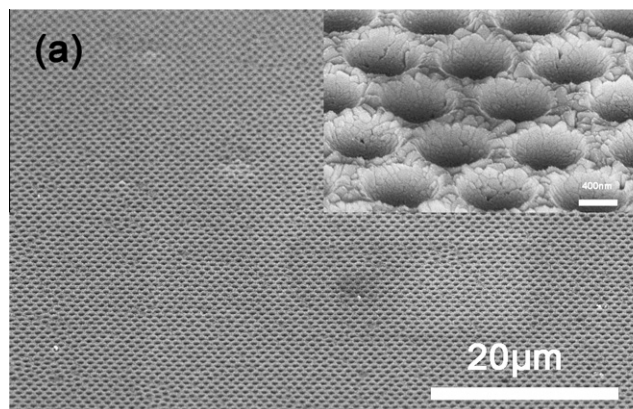
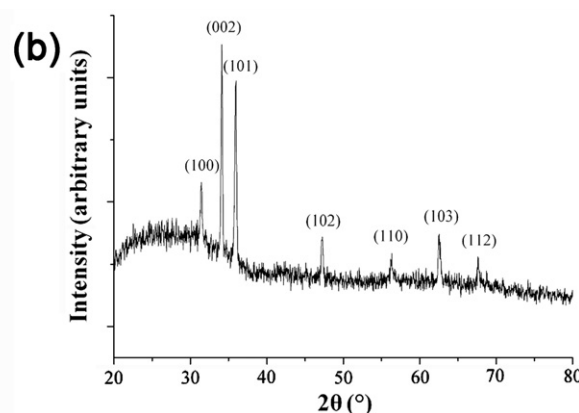
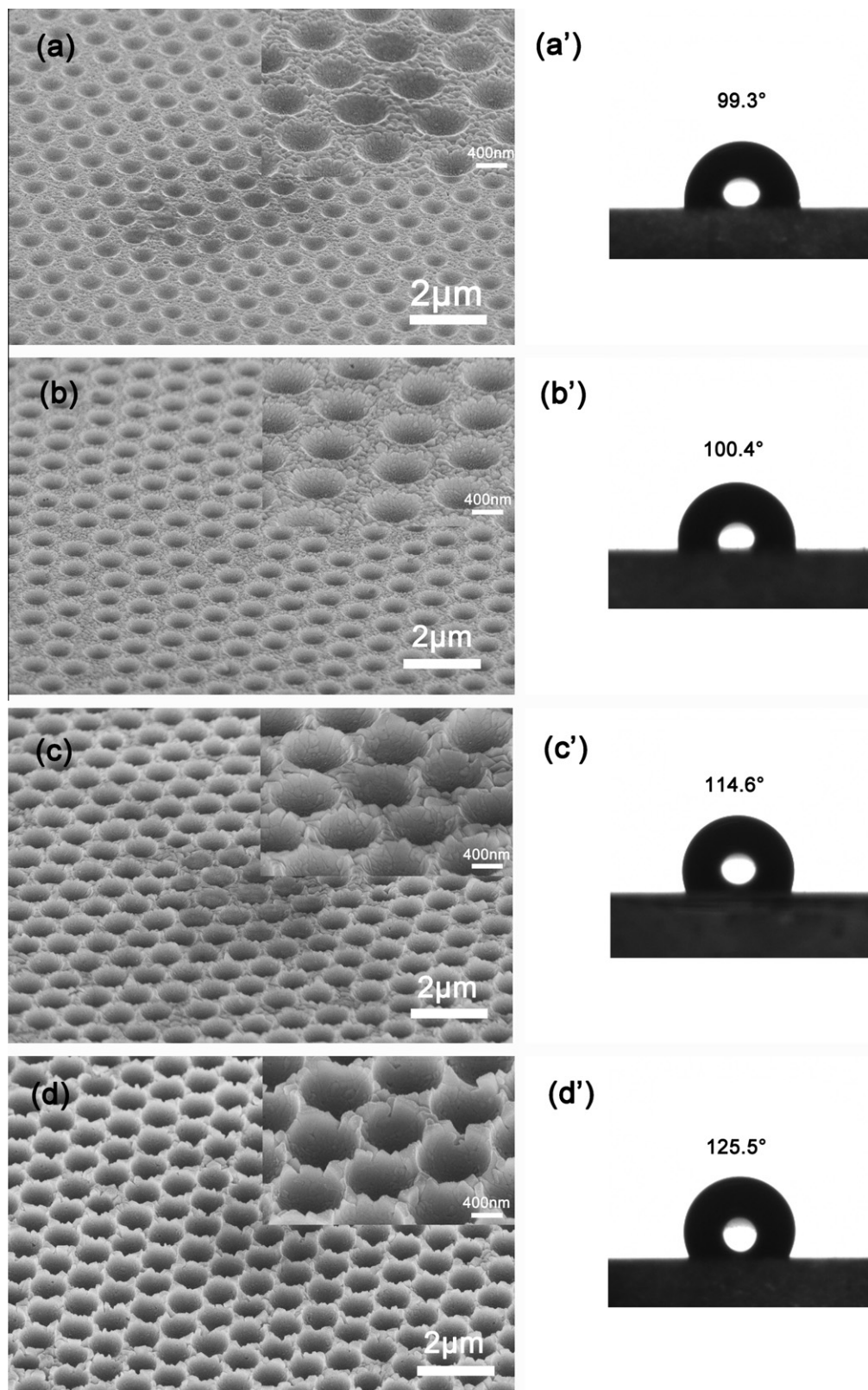


Fig. 2. SEM image and XRD pattern of a typical ZnO texture: (a) periodical ZnO textures with large-scale uniformity, the inset shows the corresponding high-magnification SEM image and (b) XRD pattern of the ZnO texture.





**Fig. 4.** SEM images and water contact angles of the periodical ZnO textures: (a–d) effect of amount of TSC on the control of growth process of periodical ZnO microbowl pattern. The TSC levels for a–d are  $0.08 \text{ mg mL}^{-1}$ ,  $0.067 \text{ mg mL}^{-1}$ ,  $0.04 \text{ mg mL}^{-1}$  and  $0.027 \text{ mg mL}^{-1}$ , respectively. The growth temperature is  $60^\circ\text{C}$  and the growth time is 12 h for all the samples; (a'–d') water contact angles for the corresponding samples with different structures.

ZnO periodical textures were fabricated by aqueous chemical synthesis with assistance of PS monolayer templates, as schematically illustrated in Fig. 1. All the growth experiments were carried out in a sealed Teflon vessel which contained 15 mL equimolar

(typically, 0.04 M was used) aqueous solution of zinc nitrate ( $\text{Zn}(\text{NO}_3)_2$ ) and hexamethylenetetramine ( $\text{C}_6\text{H}_{12}\text{N}_4$ ). A suitable amount of morphology control agent, trisodium citrate (TSC), was added to control crystal growth of ZnO. The whole growth process

lasted for 12 h at the temperature of 60 °C, and then the sample was washed with deionized water and dried under nitrogen gas stream, following to be sintered at 450 °C in the atmosphere to burn out the PS.

The synthesized samples were characterized by field emission scanning electronic microscopy (FESEM). The static CAs of water droplet was measured on a Dataphysics OCA-20 contact angle measurement system at room temperature. The volume of the water droplets used for the static CA measurements was 1  $\mu$ L.

### 3. Results and discussion

Fig. 2a shows a typical large-scale periodical ZnO texture. The ZnO arrays are uniform and display the hexagonal arrangement of bowl-like voids from the inset. The patterned ZnO films usually occupy about 2 cm<sup>2</sup> area, and exhibit iridescent color under sunlight at different angles. Fig. 2b shows the XRD pattern of the ordered ZnO texture. All diffraction peaks can be identified as diffractions from hexagonal wurtzite ZnO. It is demonstrated that the patterned ZnO film preserved polycrystalline structure. The enhanced (002) peak indicated that a strongly oriented structure was formed along (001) crystalline direction in the as-grown film.

Fig. 3 is the schematic illustration of the droplet on the textures with periodical microbowl pattern and the defined parameters. Considering of the hexagonal packing arrangement in the PS monolayer,  $f_1$  and  $\cos \theta_r$  can be roughly expressed by Eqs. (3) and (4). It can be seen that, the value of  $R$  determines the wettability of the patterned surface. It is easily deduced that the radius of the top edge of concave spherical crown ( $R$ ) and the sag height of the microbowl ( $H$ ) have the relation:  $R = \sqrt{2R_0H - H^2}$ , which means that the patterned surface with different CA can be acquired by adjusting the sag height of the microbowl.

$$f_1 = 1 - \frac{\pi}{2\sqrt{3}}(R/R_0)^2 \quad (3)$$

$$\cos \theta_r = \left[ 1 - \frac{\pi}{2\sqrt{3}}(R/R_0)^2 \right] (\cos \theta_0 + 1) - 1 \quad (4)$$

Our previous work [34–36] showed that the thickness of the ZnO film could be controlled by adding TSC and controlling the growth time. Here, we simply varied the dosage of TSC in the precursor solution to get ZnO bowl-like microbowls with various sag heights while keeping all the growth time unchanged. Fig. 4 presents the periodical ZnO bowl-like textures with different sag heights. It was found that the grown arrays changed from shallow-microbowl pattern to deep-microbowl pattern when the concentration of TSC varied from 0.08 mg mL<sup>-1</sup> to 0.027 mg mL<sup>-1</sup>, as shown in Fig. 4a–d. This is because the citrate ions are absorbed preferentially on the (0001) surface of ZnO and thus inhibit the crystal growth along the [0001] orientations [37]. The ZnO seeds layer had polycrystalline structure. As the growth carried on the ZnO crystallites began to impinge on other neighboring ones, giving rise to the competed growth of them and formation of compact film. When high concentration of TSC was used, the growth rate of ZnO crystallites was strongly suppressed. Considering that the crystal growth happened in a small confined space which was provided by the PS monolayer template and the substrate, a compact but shallow-bowl patterned ZnO film (Fig. 4a, inset) was formed. However, with TSC concentration decreasing to 0.027 mg mL<sup>-1</sup>, the growth rate of ZnO crystallites was relatively high, hence the formed microbowls (Fig. 4d, inset) became deeper than that in Fig. 4a–c (inset). Therefore, when introducing TSC into the growth of ZnO, not only a compact film was obtained, but also the sag heights of the microbowls were controlled, which is a key factor for designing definite or a series of CA in such patterned surface. The wettability of the periodical bowl-like ZnO arrays is illustrated

**Table 1**  
Theoretical Water contact angles.

Sample	$R/R_0$	$f_1$	$\theta_r$ (°)
1	0.65	0.617	114.5
2	0.69	0.568	117.5
3	0.84	0.360	131.2
4	0.90	0.266	138.4

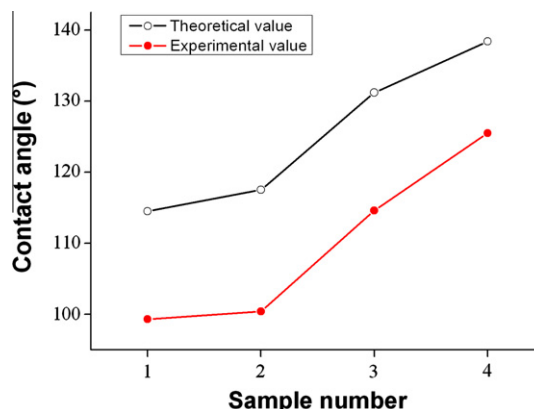


Fig. 5. Theoretical value and experimental value of  $\theta_r$ .

in Fig. 4a'–d'. The CAs of the shallow-bowl and deep-bowl pattern are 99.3°, 100.4°, 114.6° and 125.5°, respectively. Admittedly, these results indicate that the ordered porous structure can effectively change the hydrophobicity of the patterned surface through controlling the sag heights of the microbowls.

Given by the values of  $R/R_0$  (roughly measure from the SEM images of ZnO periodical textures), the theoretical  $f_1$  and  $\theta_r$  values for the four different structure surfaces have been calculated and listed in Table 1.  $\theta_0$  takes the value of 93° according to the data in Ref. [38]. The comparison between theoretical value and experimental value of  $\theta_r$  is illustrated in Fig. 5. It shows that the theoretical value is a little bit greater than the experimental one. For all that, the same trend to change surface wettability between them for diverse microbowl patterns has been clearly revealed. More attractively, when the top edge radius merely varies from 0.325  $\mu$ m to 0.450  $\mu$ m, it brings a CA variation of 26.2°. Therefore, a fine adjustment of the radii of the top edge of concave spherical-crown patterns can lead to sensitive changes of CA.

Actually, there is a difference between theoretical value and experimental value of  $\theta_r$ , which might be related with the roughness on the top zigzag surface of the solid part. Subsequently the surface wettability is affected by the shape of solid–liquid–air contact line, giving rise to a small change of CA. However, it is clear to understand that the idea is capable of changing surface wettability. More importantly, this technique combines the simplicity of self-assembly and cost benefits of wet chemical approach, which is promising for reducing the manufacturing cost of micro/nanodevices. The most prominent feature is that the synthesized structures are highly ordered. A surface with specific or quasi-continuous variation of wettability might be precisely designed in near future, which has considerable advantages in terms of potential applications in driving liquid movement.

It is worth to note that the wettability of the bowl-like surface should be mainly induced by the surface microstructure because the CAs of different ZnO crystal surfaces are nearly the same [38,39]. It means that the polycrystalline structure has little effect on the CA of solid surface. Besides, there is another point that we should pay attention to. Wenzel model [15] is also applied to

analyze the apparent CA of liquid droplet on a certain surface. It assumes that the liquid wets the whole rough surface. However, as for this ordered pattern, no matter how the radii of the top edge are modulated, the corresponding apparent CAs make little change for Wenzel state. Taking the shallowest and the deepest microbowl patterns as an example, supposing that the surface is Wenzel type, the calculated apparent CAs are about  $94.3^\circ$  and  $94.7^\circ$ , respectively. Therefore, it is not appropriate to interpret the experimental results using Wenzel model.

#### 4. Conclusion

In summary, we have succeed in synthesizing ZnO textures with well-controlled periodical microbowl pattern using a facile and effective aqueous chemical synthesis approach with the assistance of PS monolayer template. The wettability of the ZnO textures could be well modulated through fine-tuning the morphology of the microbowls. Our experimental result is consistent with theoretical calculation. The synthesis uses organic molecules to control the crystal growth and adopts a low-cost, environmentally benign wet chemical method to obtain desired structures in micro scale. Therefore, the technique for preparing such ordered periodical arrays might be used for some micro/nanodevices that are waterproof and also be extended to new applications such as self-cleaning and microfluidic devices.

#### Acknowledgment

This work was supported by the National Natural Science Foundation of China (Grant No. 10832011) and the Knowledge Innovation Program of the Chinese Academy of Sciences (Grant No. KJCX2-YW-L08).

#### References

- [1] S. Herminghaus, *Europhys. Lett.* 52 (2000) 165.
- [2] J. Bico, C. Tordeux, D. Quéré, *Europhys. Lett.* 55 (2001) 214.
- [3] N.A. Patankar, *Langmuir* 20 (2004) 8209.
- [4] W. Chen, A.Y. Fadeev, M.C. Hsieh, D. Öner, J. Youngblood, T.J. McCarthy, *Langmuir* 15 (1999) 3395.
- [5] A. Nakajima, K. Hashimoto, T. Watanabe, K. Takai, G. Yamauchi, A. Fujishima, *Langmuir* 16 (2000) 7044.
- [6] M. Li, J. Zhai, H. Liu, Y.L. Song, L. Jiang, D.B. Zhu, *J. Phys. Chem. B* 107 (2003) 9954.
- [7] L. Zhai, F.C. Cebeci, R.E. Cohen, M.F. Rubner, *Nano Lett.* 4 (2004) 1349.
- [8] J. Ji, J.H. Fu, J.C. Shen, *Adv. Mater.* 18 (2006) 1441.
- [9] P. Roach, N.J. Shirtcliffe, M.I. Newton, *Soft Matter* 4 (2008) 224.
- [10] M.K. Chaudhury, G.M. Whitesides, *Science* 256 (1992) 1539.
- [11] S. Daniel, M.K. Chaudhury, J.C. Chen, *Science* 291 (2001) 633.
- [12] J.L. Zhang, L.J. Xue, Y.C. Han, *Langmuir* 21 (2005) 5.
- [13] X. Yu, Z.Q. Wang, Y.G. Jiang, X. Zhang, *Langmuir* 22 (2006) 4483.
- [14] C.D. Bain, G.M. Whitesides, *Science* 240 (1988) 62.
- [15] R.N. Wenzel, *Ind. Eng. Chem.* 28 (1936) 988.
- [16] A.B.D. Cassie, S. Baxter, *Trans. Faraday Soc.* 40 (1944) 546.
- [17] X.S. Peng, J.P. Wang, D.F. Thomas, A.C. Chen, *Nanotechnology* 16 (2005) 2389.
- [18] J.L. Zhang, W.H. Huang, Y.C. Han, *Langmuir* 22 (2006) 2946.
- [19] X.F. Gao, L. Jiang, *Nature* 432 (2004) 36.
- [20] F. Xia, L. Jiang, *Adv. Mater.* 20 (2008) 2842.
- [21] D.L. Tian, Q.W. Chen, F.Q. Nie, J.J. Xu, Y.L. Song, L. Jiang, *Adv. Mater.* 21 (2009) 3744.
- [22] A.B.D. Cassie, *Discuss. Faraday Soc.* 3 (1948) 11.
- [23] M.H. Huang, S. Mao, H. Feick, H.Q. Yan, Y.Y. Wu, H. Kind, E. Weber, R. Russo, P.D. Yang, *Science* 292 (2001) 1897.
- [24] J.X. Wang, X.W. Sun, Y. Yang, H. Huang, Y.C. Lee, O.K. Tan, L. Vayssieres, *Nanotechnology* 17 (2006) 4995.
- [25] E. Evgenidou, I. Konstantinou, K. Fytianos, I. Poullos, T. Albanis, *Catal. Today* 124 (2007) 156.
- [26] A.B.F. Martinson, J.W. Elam, J.T. Hupp, M.J. Pellin, *Nano Lett.* 7 (2007) 2183.
- [27] Y. Qin, X.D. Wang, Z.L. Wang, *Nature* 451 (2008) 809.
- [28] T.Y. Wei, P.H. Yeh, S.Y. Lu, Z.L. Wang, *J. Am. Chem. Soc.* 131 (2009) 17690.
- [29] S.W. Kim, S. Fujita, S. Fujita, *Appl. Phys. Lett.* 81 (2002) 5036.
- [30] L. Vayssieres, *Adv. Mater.* 15 (2003) 464.
- [31] J.Y. Lao, J.Y. Huang, D.Z. Wang, Z.F. Ren, *Nano Lett.* 3 (2003) 235.
- [32] E.A. Meulenkaamp, *J. Phys. Chem. B* 102 (1998) 5566.
- [33] A. Kosiorek, W. Kandulski, P. Chudzinski, K. Kempa, M. Giersig, *Nano Lett.* 4 (2004) 1359.
- [34] D. Lan, Y.R. Wang, X.L. Du, Z.X. Mei, Q.K. Xue, K. Wang, X.D. Han, Z. Zhang, *Cryst. Growth Des.* 8 (2008) 2912.
- [35] D. Lan, Y.M. Zhang, Y.R. Wang, *Appl. Surf. Sci.* 254 (2008) 5849.
- [36] Y.M. Zhang, D. Lan, Y.R. Wang, F.P. Wang, *Front. Chem. China* 3 (2008) 229.
- [37] Z.R. Tian, J.A. Voigt, J. Liu, B. McKenzie, M.J. Mcdermott, M.A. Rodriguez, H. Konishi, H.F. Xu, *Nat. Mater.* 2 (2003) 821.
- [38] S. Yin, T. Sato, *J. Mater. Chem.* 15 (2005) 4584.
- [39] M. Miyauchi, A. Shimai, Y. Tsuru, *J. Phys. Chem. B* 109 (2005) 13307.